

Internal friction and symmetry of intrinsic point defects in GaAs

D. Laszig, H. G. Brion, and P. Haasen

*Institut für Metallphysik, Universität Göttingen, Hospitalstrasse 3/5, D-3400 Göttingen,
Federal Republic of Germany*

(Received 13 November 1990; revised manuscript received 4 March 1991)

To study the structure and symmetry of intrinsic point defects in GaAs, internal-friction measurements on *n*-type single crystals of different doping levels were performed in the range 80–440 K for a frequency of about 105 kHz. Actually, we detected damping peaks due to relaxation of point defects which are shown to be of $\langle 110 \rangle$ orthorhombic symmetry. The present analysis of the peak spectra supports an explanation in terms of midgap defect reorientations where charge-state effects seem to play a central role. The determination of the kinetic parameters of the relaxations yields activation energies of 0.6–0.8 eV for the ν_{13} and 0.85–1 eV for the ν_{12} reorientation. Remarkably large τ_0^{-1} values of 10^{18} sec^{-1} are found for the latter. They are attributed to activation entropies of the order $10k$.

I. INTRODUCTION

GaAs is currently the leading member of the III-V compound family. Therefore defect identification in this material is very important as all the electronic and atomic transport properties depend on the presence of defects. This is particularly true for intrinsic point defects that give rise to states within the forbidden gap. The existence of these defects is influenced by the mode of crystal growth and the stoichiometry.

Because of their complex behavior, a variety of experimental techniques such as deep level transient spectroscopy (DLTS) and electron paramagnetic resonance (EPR) is necessary to describe the nature of a defect, i.e., its microscopic structure. Although several aspects have been clarified recently, no clear picture concerning the configurations of point defects has been achieved yet. The controversy in the EL2 discussion impressively demonstrates this unsolved problem. None of the proposed structure models for EL2 (see, for example, Refs. 1–6) has been unanimously accepted so far. Thus, this task remains an intriguing challenge since high concentrations of EL2 in undoped bulk-grown GaAs provide enough electrons to compensate intrinsic and residual-impurity acceptors. Thereby the Fermi level is pinned in the middle of the band gap.⁷ Almost no systematic studies have been performed on the microscopic structure of other pointlike traps, among them the native donors EL3, EL5, and EL6. Consequently, none of them has been identified yet.

Internal-friction (IF) measurements as were carried out here can contribute to the structural identification of intrinsic point defects in GaAs. The IF method is sensitive to point defects which produce local elastic distortions, and, in addition, whose symmetries are lower than that of the perfect crystal.^{8,9} The advantage of IF is its capability to resolve symmetries of such defects unless their total concentration is too small. In semiconductor physics, however, IF is not widespread. The application of the IF technique was called for because several experimental re-

sults obtained by spectroscopic measurements support the view that certain deep traps in GaAs have a low symmetry.

Best candidates for IF active centers are pointlike defect complexes with a strong electron-phonon coupling. Strong electron-phonon interaction can give rise to spontaneous distortion into additional atomic configurations by lowering the symmetry, i.e., to the Jahn-Teller effect.¹⁰ This especially refers to EL2 since this donor exhibits a strong electron-phonon coupling. Its thermally activated carrier capture with an activation energy of 0.0566 eV (Ref. 11) and the value of the Huang-Rhys factor $S = 6 \pm 0.5$ (Ref. 12) indicate the existence of a non-negligible lattice distortion. The variety of phenomena associated with EL2, in particular its metastable state, has led to numerous models invoking complex defect structures. In this connection, we mention the EL6 donor frequently found in *n*-type material. From the large difference between the optical ionization energy (0.81 eV) and its thermal activation energy (0.31 eV) it was inferred that this level is a large lattice relaxation, too.¹³ In conclusion, we think it is quite reasonable to assign EL2 and EL6 to IF active point defects in GaAs.

IF measurements on GaAs are the subject of this paper. In Sec. II we provide a short introduction to the basic concepts of this technique. Subsequently, we give a summary of the defects in the samples investigated here and of the experimental details of this work. The experimental data are then described in Sec. III. Then, in Sec. IV, we analyze the IF spectra. The damping peaks give information about the structure and symmetry of the defects. The defect identification shows evidence for IF peaks due to midgap levels.

II. EXPERIMENTAL PROCEDURES AND SAMPLES

A. Experiments

IF involves a thermally activated and stress-induced ordering of point defects whose local symmetry is lower

than that of the host lattice.^{8,9} Under the influence of an applied stress the energetically equivalent defect orientations in the unstressed crystal can split. At temperatures high enough to permit motion of the defects between the various orientations, the defects will redistribute themselves among the orientations, thereby changing the strain distribution in the host lattice. Such processes are accompanied by an anelastic relaxation of the defective solid. If the relative alignment of the applied stress and defect orientation is altered, the measurable anelastic effects contribute in varying amounts, thus revealing the symmetry of the defects.

In order to observe IF, the sample is usually made to vibrate in a fundamental mode at its mechanical resonant frequency. The dissipation of energy because of defect reorientation can be detected as a damping of the vibration in the crystal. The loss of energy per cycle, Q^{-1} , for point-defect relaxation is given by the well-known Debye equation:

$$Q^{-1} = \Delta \frac{\omega\tau}{1 + (\omega\tau)^2} \quad (1)$$

In this equation, ω is the circular frequency of vibration, Δ is the relaxation strength, and τ is the time for defect reorientation expressed by an Arrhenius equation of the form

$$\tau = \tau_0 \exp(U/kT) \quad (2)$$

U is the enthalpy of activation for defect motion, k is the Boltzmann constant, and T is the temperature. The constant τ_0 is related to the lattice vibration frequency ν_0 of the defect and an entropy factor:

$$\tau_0^{-1} = \nu_0 \exp(\Delta S/k) \quad (3)$$

where ΔS is a vibrational entropy of activation. The importance of such a relation (2) is that the quantity τ may be varied over a wide range simply by changing the temperature. Thus, the peak is traced out while keeping ω fixed. The magnitude of the relaxation strength Δ , i.e., the height of the peak, in single crystals of different orientations provides information about the symmetry of the relaxing defects.

The following expression for Δ is obtained, when the stress is applied either along the $\langle 100 \rangle$ or $\langle 111 \rangle$ crystallographic direction:⁸

$$\Delta = \frac{\alpha E c_0 v_0 (\delta\lambda)^2}{kT} \quad (4)$$

where E is the appropriate Young's modulus, c_0 is the molar defect concentration, and v_0 is the atomic (or molecular) volume. The product $c_0 v_0$ is a measure of the strained portion of the specimen. $\delta\lambda$ is a dimensionless quantity describing the difference in local strain around the defect in different directions. α is a geometrical constant which depends on the symmetry of the defect and the crystallographic direction of the applied force.

Our IF measurements were carried out by the composite oscillator technique which is described in detail elsewhere.¹⁴ We used the longitudinal vibration mode at a frequency of 105 ± 2 kHz. Unfortunately, we cannot

change the frequency without a radical change of the specimen dimensions. The strain amplitude ϵ was 2.5×10^{-6} . For the glue that is necessary to couple the piezoelectric transducer to the specimen, we obtained best results with Devcon "5 minute" Epoxy (supplied by Devcon Corporation) though it put the limit of the high-temperature measurements to about 440 K. As a consequence, the investigated temperature range was between 80 and 440 K.

B. Samples

As it is common practice for the detection of point-defect relaxations, we cut rectangular bars from GaAs crystals with the long axes along the $\langle 100 \rangle$, $\langle 110 \rangle$, and $\langle 111 \rangle$ directions. For a vibration frequency of 105 kHz the lengths were 19.1 mm for the $\langle 100 \rangle$, 22.4 mm for the $\langle 110 \rangle$ - and 24.6 mm for the $\langle 111 \rangle$ -oriented samples, respectively. The cross section was 3.1×3.1 mm² for all orientations.

Three different types of n -type GaAs, all grown by the LEC (liquid encapsulated Czochralski) method (supplied by Wacker-Chemitronic), have been studied. Their doping and electrical properties at room temperature (free carrier concentration n and their mobility μ) are Te-doped ($n = 4 \times 10^{16}$ cm⁻³, $\mu = 5000$ cm²/V sec), undoped ($n = 10^{15}$ cm⁻³, $\mu = 5000$ cm²/V sec), and undoped semi-insulating GaAs ($n = 10^7$ cm⁻³, $\mu = 7000$ cm²/V sec).

For IF measurements it is of paramount importance to know as much as possible about the spectrum of defects embedded in the material that could give rise to IF peaks. Firstly, we state that the densities of grown-in dislocations, varying from 10^3 to 10^5 cm⁻², are too low to produce significant IF effects as has been proven for germanium crystals.¹⁵ Because the principal impurities found in LEC GaAs, which are carbon, silicon, and boron, are known to occupy substitutional sites of lattice symmetry, there is no need to take them into account here. This is even true for isolated antisite defects with tetrahedral symmetry and isolated interstitials on tetrahedral or hexagonal sites.

In our case, it makes sense to assign an IF peak which arises from point-defect relaxation to EL2, provided the same peak occurs in all the investigated materials as EL2 is observed in concentrations in the 10^{16} cm⁻³ range in all these crystals. Secondly, as a result of its considerable electron-phonon interaction, we note that (at least at room temperature) the charge state of EL2 is neutral in all our samples. For deep levels like EL2, one is aware that the electronic occupancy determines the structure of the defect itself and that of the lattice which surrounds it. An interpretation of point-defect relaxations in the Te-doped n -type GaAs might differ from the former pattern because it should include the EL6 donor. Non-negligible EL6 concentrations about 2.5×10^{15} cm⁻³ have been detected by DLTS measurements in this material.¹⁶ Anyway, IF peaks in GaAs grown by the LEC method might originate from the presence of vacancy defects of various configurations. The concentration of grown-in vacancies, either V_{As} or V_{Ga} , are both estimated to be in the range 10^{17} cm⁻³.¹⁷

Before and during the IF measurements the GaAs crystals were kept in the dark, to eliminate contributions to IF from interactions of deep centers with sub-band-gap light.

III. EXPERIMENTAL RESULTS

The investigation of the low-temperature range was not successful inasmuch as no point-defect relaxations were found there at all. Therefore, we restrict the presentation of the damping curves to those measured at temperatures above 290 K.

For semi-insulating *n*-type GaAs, the IF curves of an

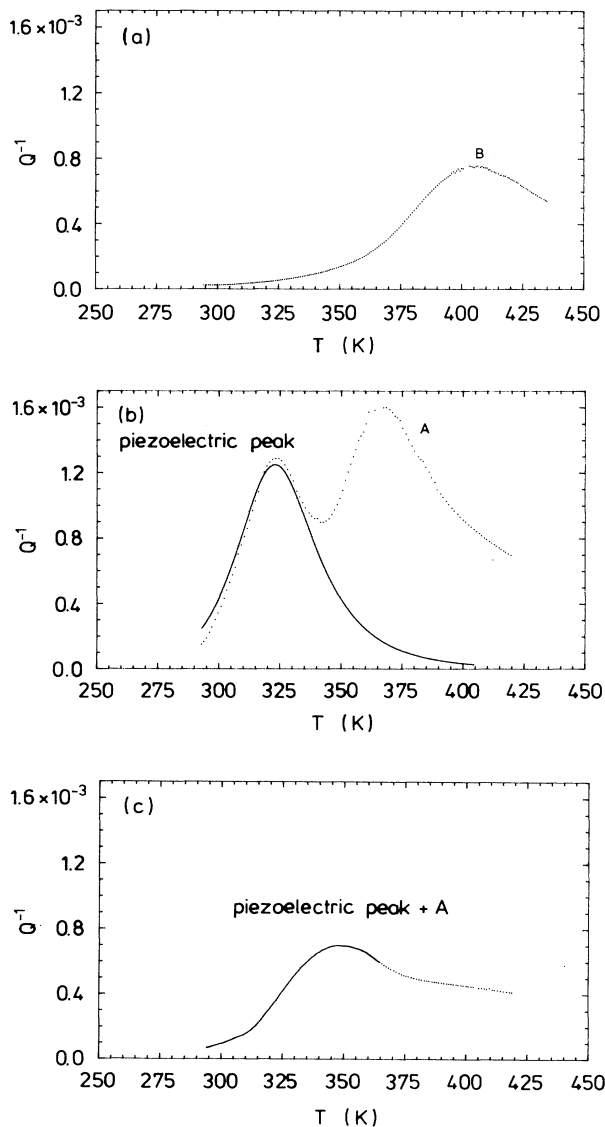


FIG. 1. Internal-friction peaks in semi-insulating *n*-type GaAs for (a) a $\langle 100 \rangle$ -, (b) a $\langle 110 \rangle$ -, and (c) a $\langle 111 \rangle$ -oriented sample, tested at 105 kHz. The curves (b) and (c) are split; the part drawn as a solid line shows the fitted piezoelectric-effect peak (b) and roughly marks its temperature range (c), respectively.

$\langle 100 \rangle$ -, and $\langle 110 \rangle$ -, and an $\langle 111 \rangle$ -oriented specimen are shown in Figs. 1(a), 1(b), and 1(c). The peaks drawn as solid lines [Figs. 1(b) and 1(c)] are not due to point-defect relaxations. As they have been studied before,^{18,19} we treat their origin only briefly at this point. These peaks arise exclusively in the piezoelectrically active $\langle 110 \rangle$ - and $\langle 111 \rangle$ -oriented high-resistivity crystals. It has been suggested that the redistribution of carriers ionized thermally from deep levels, i.e., EL2 in our crystals, to compensate the piezoelectric field accounts for the relaxation. Sufficiently high densities of free carriers suppress this effect. Since the relaxation process is controlled by thermal emission from EL2 with activation parameters of $(4 \pm 1) \times 10^{-16}$ sec for τ_0 and 0.66 ± 0.03 eV for the activation energy, the maximum damping of these piezoelectric-effect peaks is localized at temperatures between 325 and 350 K for vibration frequencies of about 105 kHz. A more comprehensive discussion of these phenomena is given by Mitrokhin *et al.*¹⁸ and Laszig and Haasen,¹⁹ so we concentrate now on the other damping peaks. Figure 1(a) shows a peak at 405 K which was observed in $\langle 100 \rangle$ oriented samples of semi-insulating (si)-GaAs. In the $\langle 110 \rangle$ direction a maximum of twofold amplitude was measured [Fig. 1(b)]. Compared to the $\langle 100 \rangle$ peak, its width is narrower by about 30 K while the maximum temperature is shifted to 367 K. The high-temperature decay of the peak is smeared out and exceeds the expected increase of the background at these temperatures. It is reasonable to interpret this high- T shoulder as an overlap with a second-smaller peak at about 405 K, which itself is not resolved. Figure 1(c) shows the damping curve for the $\langle 111 \rangle$ -oriented specimen. The peak at about 370–380 K appears only as a shoulder on the high-temperature side of the larger piezoelectric-effect peak. Due to its comparatively smaller height the resolution is limited. The high- T extension of the shoulder still allows for two Debye peaks.

Leaving aside small differences with regard to the maximum temperatures and with the peak heights collectively reduced by a factor 2, we found the same IF spectrum (without piezoelectric-effect peaks) in our undoped low-resistivity *n*-type GaAs.

In the Te-doped crystals for each orientation two peaks were clearly detected though their resolution is impaired by their close superposition. The IF spectra of correspondingly oriented samples are presented separately in Figs. 2(a), 2(b), and 2(c). The maximum temperatures for the two peaks in $\langle 110 \rangle$ - and $\langle 111 \rangle$ -oriented crystals are at about 355 and 380 K for both orientations, though the relaxation strength is anisotropic. The peaks are roughly three times as large in a $\langle 110 \rangle$ - as in a $\langle 111 \rangle$ -oriented sample. The peak temperatures of the $\langle 100 \rangle$ maxima are located near 380 K and 430 K, respectively. One recognizes their considerably larger widths (~ 50 – 60 K) compared to the ones of the $\langle 110 \rangle$ and $\langle 111 \rangle$ maxima.

For a quantitative analysis of the point-defect relaxations, i.e., for the calculation of the preexponential factors τ_0^{-1} and the activation enthalpies, we exploit the peaks' Debye shape. As will be shown later this assumption will be justified by the good agreement of such a fit with the experimental data. For a single Debye relaxa-

tion the activation enthalpy is obtained from the measured maximum temperature T_{\max} and the width ΔT of the peak at half maximum. The relation is^{8,9}

$$U = 2.63k \frac{T_{\max}^2}{\Delta T}. \quad (5)$$

Inserting U into the Eq. (2) with $\omega\tau=1$ at the peak, one gets the preexponential factor τ_0^{-1} .

According to their orientation dependence and the values for τ_0^{-1} and U , it is convenient to distinguish between two classes of peaks here. They are denoted as A and B . Group A contains merely the narrow $\langle 110 \rangle$ and

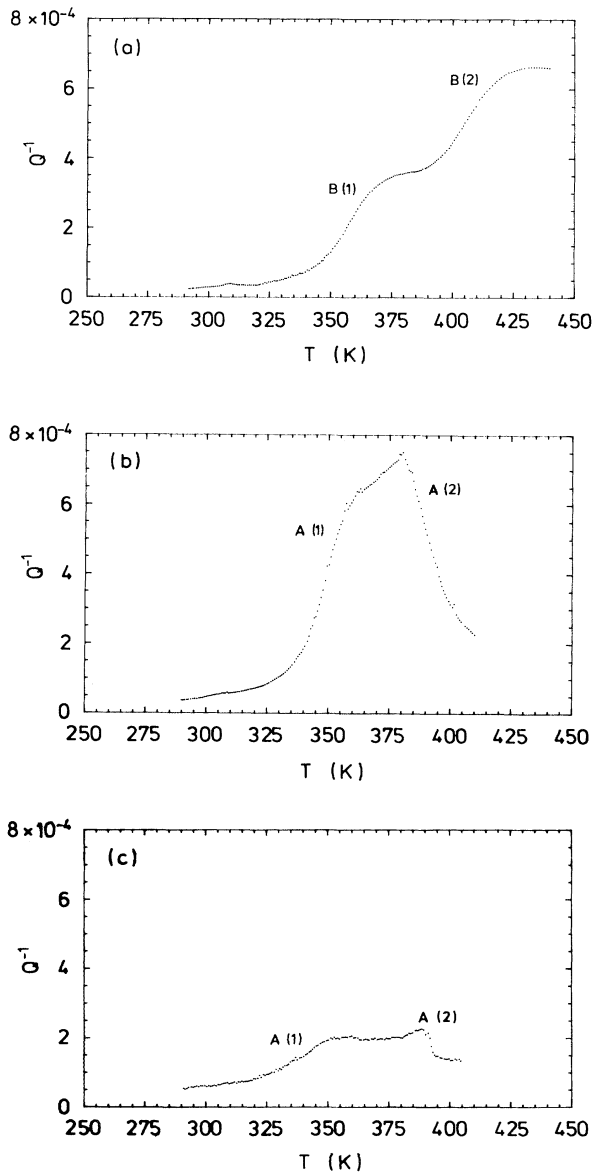


FIG. 2. Internal-friction spectra in Te-doped n -type GaAs crystals oriented in the (a) $\langle 100 \rangle$, (b) $\langle 110 \rangle$, and (c) $\langle 111 \rangle$ directions, as measured at 105 kHz.

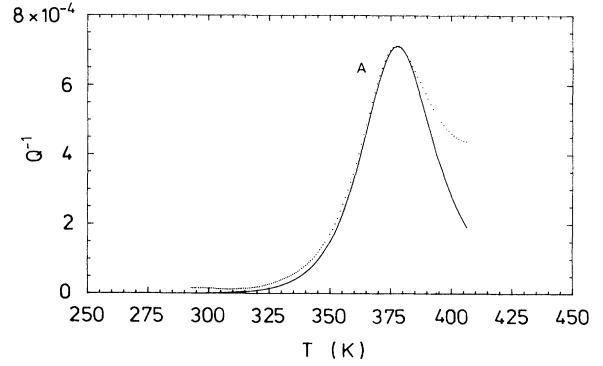


FIG. 3. Internal-friction curve of a $\langle 110 \rangle$ undoped n -type GaAs crystal (dotted line) with a peak at 377.5 K, as measured at 105 kHz; the fitted curve (solid line) is a single Debye peak for an activation energy of 0.92 eV and a prefactor of $1.34 \times 10^{18} \text{ sec}^{-1}$.

$\langle 111 \rangle$ damping maxima below 400 K. Their parameters are

$$U_A = 0.85 - 1 \text{ eV},$$

$$\tau_{0,A}^{-1} = 10^{18 \pm 1} \text{ sec}^{-1}.$$

The fundamental quantities τ_0^{-1} and U for the wide peaks of class B at around 400 K which were clearly resolved in $\langle 100 \rangle$ -oriented samples (including the $\langle 100 \rangle$ peak at about 380 K in the Te-doped samples) turn out to be

$$U_B = 0.6 - 0.8 \text{ eV}$$

$$\tau_{0,B}^{-1} = 10^{14 \pm 1} \text{ sec}^{-1}.$$

As a consistency check, the Debye curves belonging to the experimentally determined values are calculated and compared with the experimental peaks. Except for small deviations (caused by the background damping), the agreement is excellent. This fact is exemplarily demonstrated in Fig. 3 for an IF peak of a $\langle 110 \rangle$ -oriented undoped low-resistivity specimen although the peak's high-temperature side lacks resolution. The latter effect is just the same for the $\langle 110 \rangle$ maximum at 367 K in semi-insulating samples [see Fig. 1(b)]. Especially for the A peaks, it is worth emphasizing that one cannot fit the observed maxima with any different combinations of U and τ_0^{-1} .

IV. DISCUSSION AND CONCLUSIONS

For the different doping levels, all peaks of group A and B show exactly the same orientational anisotropy. Within A and B , respectively, the peaks are located in the same temperature range, and actually, their activation parameters are of the same order of magnitude. Because of these correlations, there is strong evidence that the same defect is responsible for the peaks of group A . Identical conclusions hold for the B peaks. In the following we will show that the peaks of A and B are due to the two reorientation modes of only one $\langle 110 \rangle$ orthorhombic point defect.

From the three highest defect symmetries which give rise to anelasticity in cubic crystals, tetragonal and trigonal symmetry must be excluded. With trigonal defects the largest peak heights should be observed for $\langle 111 \rangle$ -oriented samples. In principle, trigonal point defects do not reorient under a $\langle 100 \rangle$ -oriented stress. For tetragonal defect symmetry the largest relaxation maxima should be measured for $\langle 100 \rangle$ -oriented single crystals, and the relaxation effect should nearly vanish for a stress in the $\langle 111 \rangle$ direction. Above all, for both defect symmetries there should be only one independent reorientation frequency. Consequently, for a defect of trigonal or tetragonal symmetry one should find a peak temperature that is nearly unaffected by changes of the stress axis. As a matter of fact our peaks do not fulfill these requirements. $\langle 110 \rangle$ orthorhombic symmetry is compatible with the heights of the peaks belonging to class A. They are about three times larger for $\langle 110 \rangle$ - than for $\langle 111 \rangle$ -oriented specimens. The reason for the absence of group A peaks in $\langle 100 \rangle$ stress experiments is the existence of two independent reorientation frequencies for $\langle 110 \rangle$ orthorhombic defects. Conventionally, one denotes the rate at which a defect along $\langle 110 \rangle$ turns into $\langle 1\bar{1}0 \rangle$ with ν_{12} while ν_{13} stands for the rate for the jumps into the other principal orientations. For illustration, it is sufficient to introduce the relaxation rates for stresses applied along the $\langle 100 \rangle$ and $\langle 111 \rangle$ directions.^{8,9}

$$\tau_{\langle 100 \rangle}^{-1} = \nu_{13} ,$$

$$\tau_{\langle 111 \rangle}^{-1} = 2\nu_{12} + 4\nu_{13} .$$

The two relaxation processes are depicted in Fig. 4 (for simplicity, we have chosen a defect pair in a fcc lattice). It is important to note that under a $\langle 100 \rangle$ uniaxial stress only the ν_{13} reorientation occurs, but both processes are allowed when stress is applied to $\langle 110 \rangle$ - and $\langle 111 \rangle$ -oriented samples.^{8,9} Considering these preliminaries, it can be understood that the A peaks result from the ν_{12} reorientation while the B peaks are due to the ν_{13} relaxation mode. The superposition of these two relaxations

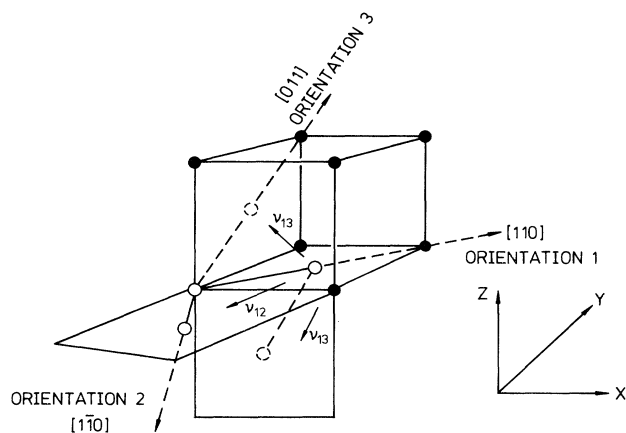


FIG. 4. Illustration of the reorientation frequencies ν_{12} and ν_{13} for a $\langle 110 \rangle$ orthorhombic nearest-neighbor defect pair in the fcc lattice.

accounts for the origin of the shoulders on the high-temperature sides of the A peaks as they are very clear in the $\langle 110 \rangle$ -oriented semi-insulating and low-resistivity undoped crystals [see Figs. 1(b) and 3].

Obviously, the Te-doped material is exceptional since the IF of a second $\langle 110 \rangle$ orthorhombic defect is added to the peak spectrum. However, the two A peaks and the two B peaks are too similar in every respect to decide unambiguously whether the ones with lower or those with higher maximum temperatures are the relaxations of this second point defect.

Next, we attempt an interpretation of the high τ_0^{-1} values of the ν_{12} reorientation. Values about 10^{18} sec^{-1} are anomalously large and exceed the Debye frequency by five orders of magnitude. Nevertheless comparably high τ_0^{-1} values are known.²⁰ Because atomic movements with such frequencies must be excluded, we turn our attention to the entropy factor in Eq. (3). ΔS corresponds to the entropy difference between two states, one in which the reorienting defect is in its saddle point, the other in which the defect is in one of its equilibrium positions. To explain 10^{18} sec^{-1} in terms of ΔS , entropy values within the range of $10k$ are required. For comparison, similar values of the self-diffusion entropy of a vacancy in germanium have been derived by Seeger and Chik²¹ as an explanation of the large preexponential factors. They suggested that this large entropy arises from a spreading out of the vacancy over several atomic volumes. Our interpretation of a large reorientational entropy for the defects follows Seeger and Chik insofar as we argue that the change of its axis from $\langle 110 \rangle$ into $\langle 1\bar{1}0 \rangle$ involves an appropriate spreading out of the defect and a strong lattice distortion around it. Similar high values for ΔS which may vary with temperature have been derived by Lannoo and Bourgoin.¹⁰ The situation is quite different for the ν_{13} relaxation. With values of $10^{14 \pm 1} \text{ sec}^{-1}$, there is no evidence for a large reorientational entropy. The latter conclusion is consistent with the fact that for most $\langle 110 \rangle$ orthorhombic defects the ν_{13} reorientation is achieved by one nearest-neighbor jump, e.g., see Fig. 4, whereas the process for the ν_{12} reorientational mode appears to be more complicated.

At a lower frequency (13.9 kHz) and much earlier Chakraverty and Dreyfus²² measured in GaAs of the then available purity two damping peaks, one at 360 K and the other at 403 K. Both peaks did not always occur. The low-temperature one appeared upon initial heating whereas the other one was observed upon cooling. As soon as the specimen had been kept for some hours at 620 K only the high-temperature peak was found to be stable. The latter one shows an apparent coincidence with our maximum at 403 K, although measured at different frequencies (13.9 and 105 kHz). The activation enthalpy is equal, whereas the τ_0^{-1} differs by a factor 10. The defect symmetry that fits their experimental results is also orthorhombic. Due to its irreproducible behavior upon subsequent heat treatment the other damping peak is not discussed by the authors.

Because of changes in the peak height by heat treatment of the specimen in arsenic vapor Chakraverty and Dreyfus conclude that their peak is not related to impuri-

ties but to an intrinsic defect. They assume for it the re-orientation of bound pairs of Ga vacancies. For defects in GaAs the latter statement cannot be maintained any more. It is generally accepted,²³ that either As interstitials or As antisites account for the nonstoichiometric, As-rich composition of GaAs. Both defects change their concentration during heat treatment in arsenic pressure.

By this process maximum concentrations of $5 \times 10^{16} \text{ cm}^{-3}$ can be reached for EL2. These new findings support our opinion to assign our peaks to EL2.

For a peak height of $Q^{-1} = 0.8 \times 10^{-3}$ [Fig. 1(a)] the quantity $\delta\lambda$ can be estimated according to Eq. (4). In our case the quantity v_0 has to be assumed larger than the molecular volume. The EL2 model of Figielski⁴ involving two antisites and one interstitial has a $\langle 110 \rangle$ orthorhombic symmetry. It is reasonable to assume v_0 in the order of at least one unit cell. With $\alpha = 2/9$ (Ref. 8) $E_{\langle 110 \rangle} = 8.5 \times 10^6 \text{ N cm}^{-2}$ and $c_0 = 2 \times 10^{-6}$ one obtains $\delta\lambda = 0.8$. This is a large value representing a severe lattice distortion but still acceptable.

IF measurements on *n*-type semi-insulating GaAs at a frequency of 6.8 kHz, performed by Mitrokhin *et al.*,¹⁸ show only the large EL2 piezoelectric-effect peak ($Q_{\text{max}}^{-1} \sim 10^{-3}$), but not our peaks. We must ask why our point-defect relaxations are absent there. Assuming constant activation parameters in semi-insulating crystals, the ν_{12} ($U = 0.95 \text{ eV}$, $\tau_0^{-1} = 8.37 \times 10^{18} \text{ sec}^{-1}$) and ν_{13} ($U = 0.6 \text{ eV}$, $\tau_0^{-1} = 2 \times 10^{13} \text{ sec}^{-1}$) reorientations should be observed at 336 K and 349 K, respectively, when the vibration frequency is 6.8 kHz. Therefore, it needs to be explained why the defects do not reorient at these lower temperatures. An approach to reconcile our results with the damping curves of Mitrokhin *et al.* and our earlier measurements at 50 kHz must be based on defect properties which change within the temperature range between 335 and 400 K. Transformations of defect structures are not known to occur in the temperature range of our IF peaks, so we turn our attention to the exponentially increasing thermal emission of electrons from occupied deep levels like EL2 to the conduction band. Thus, we compare the thermal electron emission rates of EL2 (see, for example, Ref. 23) at the maximum temperatures for 105 kHz (367 K for the ν_{12} and 405 K for the ν_{13} peak) with those at 336 and 349 K. In fact, the resulting ratios are about 13 and 58, respectively. These large differences suggest that the observed relaxations might be due to reorientations of deep level defects which are affected by changes of charge state as they are specific to defect migration in semiconductors.¹⁰ Due to a high impurity content in the order of 10 ppm (Al, Si, O) in the GaAs used by Chakraverty and Dreyfus the charge state of EL2 and other deep level defects may be completely different from that in our specimens. The change of the peak formation upon thermal cycles in their specimens indicate that the material was not thermally stabilized. Even the state reached after their heat treatment at 670 K may be an intermediate one. Further tempering at higher temperatures would shift their peaks again. Though the exact thermal stabilization process is not known, it needs a temperature treatment above 1000 K.

The most probable intrinsic point defect that fits the

experimental results of our peaks is a complex defect which is related to a deep level.²⁴ One recognizes that our damping maxima meet the main conditions for EL2 IF peak discussed in Sec. II, and its predominant position as a point defect in practically all our materials is generally accepted. This defect identification, however, is in serious contradiction to a microscopic model that describes EL2 simply as an antisite As_{Ga} and which has been proposed by Dabrowski and Scheffler⁵ and Chadi and Chang.⁶ Equally, $\langle 110 \rangle$ orthorhombic defect symmetry is not consistent with the EL2 model of a trigonal distant $\text{As}_{\text{Ga}}\text{-As}_i$ pair with an As interstitial As_i on a tetrahedral site. The latter model is the most investigated and discussed one.^{1,2} Recently, Bourgoin *et al.*²³ and Kamrock *et al.*²⁵ extended the $\text{As}_{\text{Ga}}\text{-As}_i$ model by adding an antisite Ga_{As} . From our point of view, this picture is not satisfying since the position of the Ga_{As} and, therefore, the symmetry of the complete configuration remain unsolved. However, the EL2 model given by Figielski and Wosinski⁴ has the symmetry suggested by our experiments. Their EL2 center model is a complex defect composed of two As antisites aligned along a $\langle 110 \rangle$ axis in the second-neighbor configuration plus an As interstitial in between on a tetrahedral site. A full discussion of the degree of agreement of this EL2 model with our experimental results cannot be given here. On the basis of our IF data alone, the identity of the second defect in the Te-doped crystals cannot be elucidated. Apart from a high concentration of EL6, we must also take into consideration experimental indications for the existence of a whole EL2 defect family. Partly, the concept of an EL2 family has been developed to explain the sample dependence of the thermal and the photoinduced recovery of photoquenched EL2.^{26,27} Apart from looking at EL2 and EL6, it has been shown that *n*-type Te-doped samples contain a high concentration of vacancy defects.²⁸ So, these defects cannot be excluded here. Consequently, the identity of this second $\langle 110 \rangle$ orthorhombic defect remains ambiguous. According to the existence of such vacancy defects like the $\text{As}_{\text{Ga}}\text{-V}_{\text{Ga}}$ complex¹⁷ of $\langle 110 \rangle$ orthorhombic symmetry, the latter admission even refers to the identity of the first $\langle 110 \rangle$ orthorhombic defect.

As a summary, we state that for a determination of the microscopic structure of intrinsic point defects in GaAs the IF technique is useful. The results for *n*-type LEC GaAs suggest the relaxation of complex midgap centers of $\langle 110 \rangle$ orthorhombic defect symmetry. Since the damping peaks are observed only at temperatures high enough to permit significant thermal emission from EL2 and other deep levels, this might be an indication that the relaxations are controlled by a charge-state effects. We ascribe a prefactor τ_0^{-1} of about 10^{18} sec^{-1} , measured for the jumps that take the defect from $\langle 110 \rangle$ to $\langle 1\bar{1}0 \rangle$, to a reorientational entropy of $10k$.

ACKNOWLEDGMENTS

The authors are indebted to H. J. von Bardeleben and J. C. Bourgoin (Paris) for their critical reading of the manuscript and their specific suggestions for improving it. This work has been supported by the Deutsche Forschungsgemeinschaft (Bonn, Germany).

- ¹H. J. von Bardeleben, D. Stievenard, D. Deresmes, A. Huber, and J. C. Bourgoin, *Phys. Rev. B* **34**, 7192 (1986).
- ²B. K. Meyer, D. M. Hoffmann, J. P. Niklas, and J.-M. Spaeth, *Phys. Rev. B* **36**, 1332 (1987).
- ³J. F. Wager and J. A. van Vechten, *Phys. Rev. B* **35**, 2330 (1987).
- ⁴T. Figielski and T. Wosinski, *Phys. Rev. B* **36**, 1269 (1987).
- ⁵J. Dabrowski and M. Scheffler, *Phys. Rev. B* **40**, 10391 (1989).
- ⁶D. J. Chadi and K. J. Chang, *Phys. Rev. Lett.* **60**, 2187 (1988).
- ⁷E. J. Johnson, J. A. Kafalas, and R. W. Davies, *J. Appl. Phys.* **54**, 204 (1983).
- ⁸A. S. Nowick and B. S. Berry, *Anelastic Relaxation in Crystal-line Solids* (Academic, New York, 1972).
- ⁹R. de Batist, *Internal Friction of Structural Defects in Crystal-line Solids* (North-Holland, Amsterdam, 1972).
- ¹⁰For a comprehensive review, see M. Lannoo and J. C. Bourgoin, *Point Defects in Semiconductors, I—Theoretical Aspects* (Springer, Berlin, 1981); J. C. Bourgoin and M. Lannoo, *Point Defects in Semiconductors, II—Experimental Aspects* (Springer, Berlin, 1983).
- ¹¹A. Mitonneau, A. Mircea, G. M. Martin, and D. Pons, *Rev. Phys. App.* **14**, 853 (1979).
- ¹²S. Makram-Ebeid and M. Lannoo, *Phys. Rev. B* **25**, 6406 (1982).
- ¹³A. Chantre, G. Vincent, and D. Bois, *Phys. Rev. B* **23**, 5335 (1981).
- ¹⁴R. B. Schwarz, *Rev. Sci. Instrum.* **48**, 111 (1977).
- ¹⁵U. Jendrich, Ph.D. thesis, Universität Göttingen, 1988; *Phys. Status Solidi A* **108**, 553 (1988).
- ¹⁶T. Wosinski and T. Figielski, *Solid State Commun.* **63**, 885 (1987).
- ¹⁷S. Dannefaer and D. Kerr, *J. Appl. Phys.* **60**, 591 (1986).
- ¹⁸V. I. Mitrokhin, S. I. Rembeza, V. V. Sviridov, and N. P. Yaroslavtsev, *Phys. Status Solidi A* **119**, 535 (1990).
- ¹⁹D. Laszig and P. Haasen, *Phys. Status Solidi A* **104**, K105 (1987).
- ²⁰J. B. Wachtman and L. R. Doyle, *Phys. Rev.* **135**, A276 (1964).
- ²¹A. Seeger and K. P. Chik, *Phys. Status Solidi* **29**, 455 (1968).
- ²²B. K. Chakraverty and R. W. Dreyfus, *J. Appl. Phys.* **37**, 631 (1966).
- ²³J. C. Bourgoin, H. J. von Bardeleben, and D. Stievenard, *J. Appl. Phys.* **64**, R64 (1988).
- ²⁴M. Hoinkis, E. R. Weber, W. Walukiewicz, J. Lagowski, M. Matsui, H. C. Gatos, B. K. Meyer, and J. M. Spaeth, *Phys. Rev. B* **39**, 5538 (1989).
- ²⁵K. Kambrock, B. K. Meyer, and J.-M. Spaeth, *Phys. Rev. B* **39**, 1973 (1989).
- ²⁶D. W. Fischer, *Phys. Rev. B* **37**, 2968 (1988).
- ²⁷J. C. Parker and R. Bray, *Phys. Rev. B* **37**, 6368 (1988).
- ²⁸C. Corbel, F. Pierre, P. Hautojärvi, K. Saarinen, and P. Moser, *Phys. Rev. B* **41**, 10632 (1990).